Atmospheric and Climate Data: Aerosol Light Scattering as a Function of Atmospheric and Climate Parameters

Siyao Cui, Kunjie Fan, Hanyang Li, Guanqian Wang, and Qi Zhao

1. Introduction and motivation

Aerosols are collections of tiny particles of solid and/or liquid suspended in the atmospheric (Mukai et al., 2006). They directly affect the Earth's climate by absorbing and scattering solar radiation, which results in both heating and cooling of the climate system. The net contribution of aerosols to climate effect has been estimated to be -0.9 W m^{-2}, which is opposed to the positive climate effect by greenhouse gases (2.63 W m^{-2}) (Cappa et al., 2016). Different aerosols absorb or scatter sunlight to varying degrees, depending on their optical properties. Aerosols also have adverse effects on human health and may cause cardiovascular and lung diseases (Lelieveld et al., 2015), but our primary focus will be the climate implications of aerosols in this work.

Because the fundamental understanding of the aerosols (such as their optical properties, mixing state, and lifetime in the atmosphere) is still limited, the contribution of absorbing aerosols to climate effects remains highly uncertain. For example, the uncertainty of radiative forcing associated with the aerosols is estimated to be at least a factor of three (Boucher, 2015). The uncertainty is partially due to the fact that optical measurements (such as scattering coefficients (B_s)) of aerosols are not consistently deployed in routine monitoring at many of the ground-based networks around the world, so updating the coefficients may not be trivial. **Consequently, examining the ability of various models to predict scattering by aerosols will be beneficial to understand the association between aerosol scattering and commonly-used atmospheric parameters, which in turn yields more robust results of climate effects due to aerosols.**

Fundamentally, multiple linear regression (MLR) analysis has been used to predict B_s (e.g., Malm et al., 2000; White and Roberts, 1977), using the following equation:

$$\mathbf{B_s = \Sigma\, \alpha_i\, m_i} \quad (1)$$

where α_i and m_i are the specific scattering cross section (the regression coefficients) and species concentration, respectively.

On the basis of Eq. 1, **this project aims to apply various statistical techniques to explore: 1). Is there any "natural" clusters of aerosol and climate observations and what is their relationship with B_s? 2). Is B_s a function of various aerosol characteristics and atmospheric states?** The research questions are proposed to analyze by two tasks (using a set of unsupervised learning and supervised learning techniques, respectively).

2. Dataset description and exploratory

The dataset used for this analysis is the ground-based atmospheric and climate data measured at Southern Great Plains observatory (Lamont, OK) from 01/01/13 to 12/31/13. The raw data is downloaded from the U.S. Department of Energy Atmospheric Radiation Measurement (ARM) website. The SGP observatory was the first field measurement site established by the ARM user facility. This observatory is the world's largest and most extensive climate research facility.

The data is pre-processed by averaging every 30 minutes. The dependent variable is 'B_s'. There are 13 predictors: 12 predictors are continuous variables, and one predictor is a binary variable.

We first conducted the exploratory data analysis (EDA) and found several interesting facts that relate to the two questions we want to study. For example, we found that the data of some variables are missing from 07/14/13 to 10/05/13. Consequently, we remove observations with missing values, and 7637 observations are left for analysis. Moreover, we found that 'B_s' and 'B_a' (one important predictor) have

significant difference across months for both PM1 and PM10 through boxplots, therefore we proposed to perform clustering algorithms first (see section 4.1).

Most importantly, the collinearity test of the dataset (VIF-test) provided evidence for the existence of collinearity between variables. The VIF value of 'ammonium' exceeds 10, which is a traditional indicator in statistics for collinearity. The collinearity is confirmed and addressed in our regression analysis (see section 4.3).

We also explored the influence of interactions between predictors. According to prior knowledge, interactions between 'RH' and 'nitrate' may affect response (Malm et al., 2000). We test the interaction with scatter plots, and reject the interaction between 'RH' and 'nitrate' because of the obvious unrelation in the present dataset. The interaction term included in this report is 'B_a:class', because the aerosol sampling of 'B_a' and 'B_s' was switched every 30 minutes between sub-10-micron and submicron size aerosol during the measurements. Consequently, the interaction between the binary variable (class) and 'B_a' is expected to collectively affect the prediction of 'B_s'. A more detailed description of the EDA can be found in our EDA report.

3. Methods

Here, we briefly summarize the methods we propose to use in this work, because we already presented the model design in the proposal.

Task 1. Unsupervised learning

We first explore the structure of the dataset using unsupervised learning techniques. Specially, we use PCA analysis on all the predictors and investigate the structure of the data by visualizing the first two dimensions. Certain patterns of the observations are detected in the PCA plots and the relationship between each predictor can be analyzed by looking at the PCA loadings.

Task 2. Regression Analysis

In terms of regression analysis, we decide to use the following methods to perform model selection: Best Subset Method, Forward/Backward Stepwise Method, Lasso Method, Ridge Method, and Support Vector Regression (SVR). The team split the data into training set and test set. All data are standardized and the response variable is transformed before analyzing (See section 4.2). The dataset is split into train and test set with a split ratio of 8:2. Then, the team use all above-mentioned methods to build models. Later, the team use the test set to evaluate the best models selected by each method (using test MSE).

After model selection, we analyze the residuals of the best model for diagnostics and check assumptions of the linear model. Also, we explore the effect of timing on the 'B_s' prediction, and suggest the most appropriate time series model for residuals.

4. Results and discussion

4.1. Structure of data (unsupervised learning)

We perform PCA analysis using all the predictors for PM1 and PM10 (the variable of 'class'), respectively, and we will focus on the result of PM1 in this report. The cumulative explained variance of the first two principal components is 43%. The left panel in Figure 1 shows the PCA scores of the first two components and the color indicates the '$\log(B_s)$'. As we can see from the figure, there exists a pattern ranging from the left to right where '$\log(B_s)$' is increasing, which means that the predictors are related to the response variable. In other words, the first component is strongly and positively associated with '$\log(B_s)$', but the second component seems to be weakly associated with '$\log(B_s)$'. We explore more on the loadings of each predictor later.

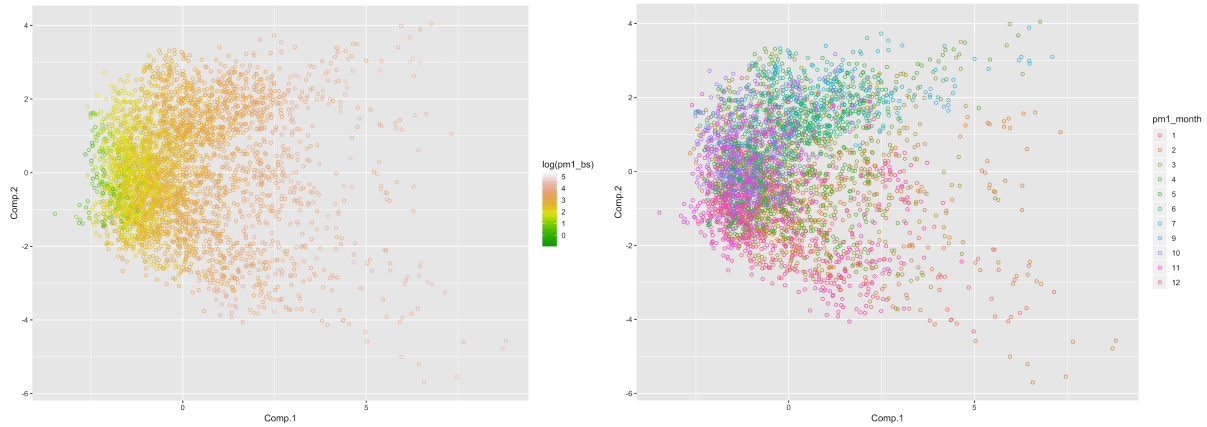

Figure 1. PCA plot where color indicates the value of log(B_s) in the left panel and month information in the right panel

In order to see whether the distribution of predictors is related to the season, we indicate the month information on the PCA score plot (the right panel in Figure 1). Hot seasons such as June, July and September can be roughly separated from cold seasons like month November, December and January. Interestingly, the seasonal pattern is more related to the second component, different from the feature in the left panel. Consequently, these interesting structures in the data motivate us to plot the biplot figure to see the relationship between each predictor indicated by the first two components.

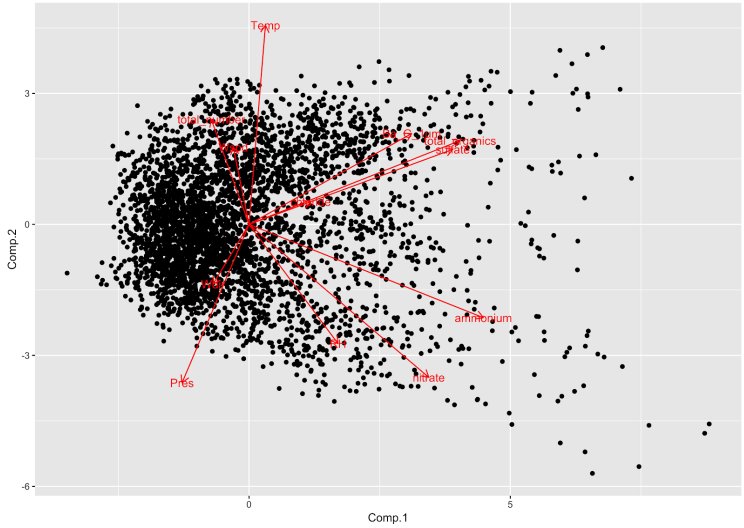

Figure 2. Biplot figure showing both PCA scores and PCA loadings

As shown in Figure 2, the first loading vector places the most weight on 'ammonium' and roughly equal weight on 'nitrate', 'total_organic', and 'sulfate'. The results are encouraging and indicate that the first component is a measure of the overall aerosol chemical characteristics. Therefore, it is not surprising that the response variable ('B_s', the variable not included in the PCA) tends to increase as PC1 increases, suggesting that these chemical properties may play important roles when predicting 'B_s'. Nevertheless, the second component places its most positive weight on 'temperature' and most negative weight on 'pressure', indicating the negative relation between 'temperature' and 'pressure'. In particular, 'temperature' and 'wind_spd' load much more strongly (almost exclusively) on PC2. We suspect that these two variables may be not significant when predicting 'B_s' using regression techniques.

4.2. Transformation

Considering that the normality is an important assumption for regression analysis, we first check the distribution of our dependent variable ('B_s').

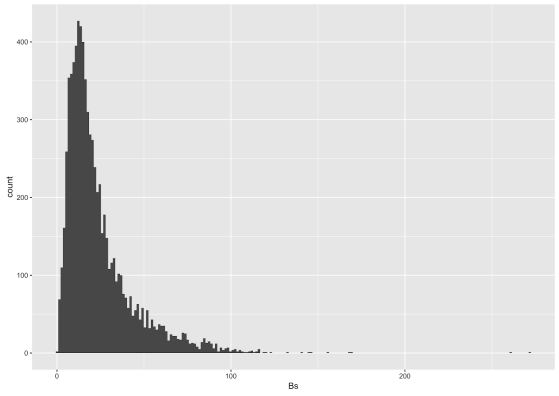

Figure 3. Distribution of original B_s value

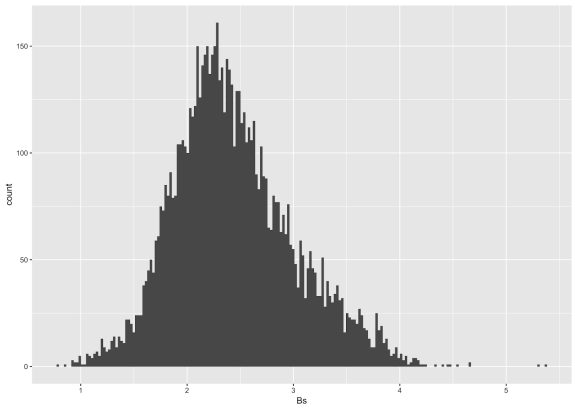

Figure 4. Distribution of transformed value of B_s

As we can see in Figure 3, the distribution doesn't confirm normality. Therefore, transformation method needs to be applied to adjust the response variable to confirm normality. Here we use Box-Cox transformation, which attempts to identify an appropriate exponent (lambda) used to transform the original data into a normal shape. The lambda value indicates the power to which all data should be raised. In our case, lambda = 0.5 gives the best transformation, as shown in Figure 4.

4.3. Model selection

Our goal is to select important factors for accurate estimation of 'B_s'. Accordingly, we construct the following seven models using what we learnt in class. Table 1 summarizes the selected variables by each model only using the training dataset.

Table 1. Summary of selected variables in all models

Best_Cp_R_sqrt	Best_BIC	Forward(BIC)	Backward(BIC)	Both_Direction(BIC)	LASSO	Ridge
ammonium	ammonium	ammonium	ammonium	ammonium	ammonium	ammonium
Ba_G	Ba_G	Ba_G	Ba_G	Ba_G	Ba_G	Ba_G
chloride	chloride	chloride	chloride	chloride	chloride	chloride
class	class	class	class	class	class	class
nitrate	nitrate	nitrate	nitrate	nitrate	nitrate	nitrate
Pres	Pres	Pres	Pres	Pres	Pres	Pres
RH	RH	RH	RH	RH	RH	RH
sulfate	sulfate	sulfate	sulfate	sulfate	sulfate	sulfate
Temp	Temp	Temp	Temp	Temp	Temp	Temp
total_number	total_number	total_number	total_number	total_number	total_number	total_number
total_organics	total_organics	total_organics	total_organics	total_organics	total_organics	total_organics
Wdir	Wdir	Wdir	Wdir	Wdir	Wdir	Wdir
Wspd	Wspd	Wspd	Wspd	Wspd	Wspd	Wspd
Ba_G:class	Ba_G:class	Ba_G:class	Ba_G:class	Ba_G:class	Ba_G:class	Ba_G:class

Coefficient is Smaller Than 0.01
Method Selected Variables
Non- Significant in Summary

From the above table, we can basically consider "pres" and "wspd" not relevant to the prediction of "B_s".

However, we also performed the analysis without including the interaction term (Ba:class). In such situation, we found that "class" is not selected by most of the models. The "class" is a binary variable which records the switched impactor in the system which toggles the aerosol cut-size between 1.0 μm (PM1) and 10 μm (PM10) aerodynamic particle diameters every 30 min. The switch is only applicable to the variables related to aerosol optical properties, including "B_s" and "B_a". As expected, the effect of "class" is expected to be well captured by "B_a" when predicting "B_s" (Also see **Figure 1 in the EDA report**). Similarly, Jefferson (2011) observed a similar pattern of SGP data for most of the days in 2010, indicating that larger supermicron aerosols that absorb and scatter light are seldom present at SGP site. This is a question we will explore besides the class project.

4.3.1. Best subset selection

In the first, we perform the 'best subset selection' by identifying the best model using RSS, adjusted R-square, Cp, and BIC. For instance, we see that the adjusted R-square statistic increases from 48%, when only one variable ('ammonium') is included in the model, to almost 80%, when 13 variables are included. We select the best subset by plotting RSS, adjusted R-square, Cp, and BIC for all of the models (Figure 5). Both the criteria of adjusted R-square and Cp tell us that the best model is the one with 13 predictor variables. However, using the BIC criteria, we should go for the model with 12 variables.

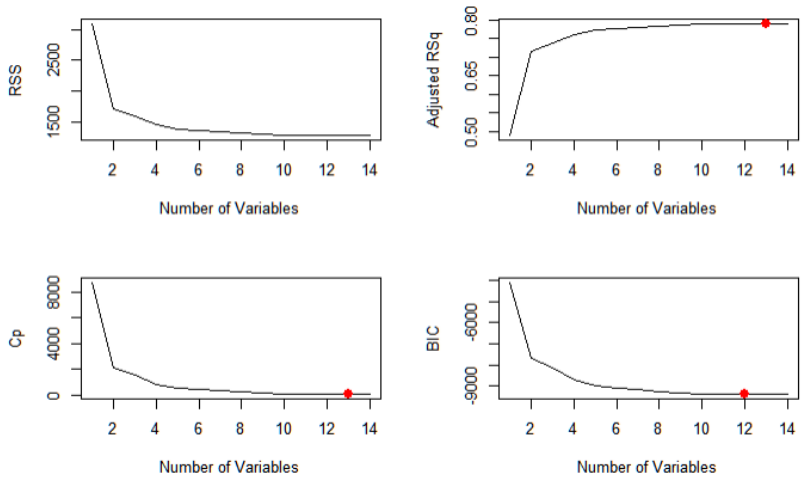

Figure 5. The best subset selection as a function of the number of variables

Compared to the model suggested by the adjusted R-square and Cp criteria (we simply call the model 'best-Cp' in the rest of the report), the discarded variable using the BIC criteria (we call the model 'best-BIC' in the rest of the report) is 'wind_spd'. In the 'best-Cp' model, the variables of 'RH' and 'wind_spd' show p-values slightly less than 0.05 and low coefficients. However, in the 'best-BIC' model, after removing 'wind_spd', the effect of 'RH' increase (p-value<0.001 and coefficient=-0.02). Considering the inherent relationship between wind speed and aerosol-related parameters (e.g., greater wind speed blows more pollution from overseas to the observational site), it is not surprising that the 'best-BIC' drops 'wind_spd' due to collinearity. Therefore, we decided to keep the 'best-BIC' model at this point.

4.3.2. Stepwise model selection

We next apply "forward", "backward", and "both" stepwise model selection. The selected best model is identical using different stepwise selection criteria, which is the same as the 'best-BIC'.

4.3.3. Lasso and ridge model selection

Another group of models we test is the Lasso and Ridge methods. Theoretically, both models do not eliminate any variables when using the lambda that minimizes the cross-validation MSE (the left lines in Figure 6). Alternatively, if we select the lambda that is the largest within one standard deviation of the MSE, in order to favor the simplicity of the model around the optimal lambda value, we get a model with 12 variables when using the Lasso method (while all variables remain in the ridge model).

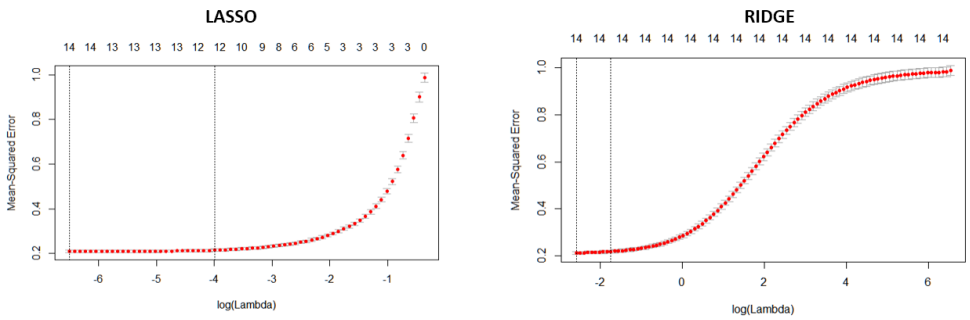

Figure 6. Cross-validated errors of regression with lasso and ridge penalty

We next assess the results derived from the Lasso method visually (Figure 7a). One may notice that ammonium is increasing with lambda for a certain range. It is most likely because it is associated with many other variables (such as nitrate, sulfate, and chloride). Consequently, when the model simplified to include only three variables, 'B_a', 'ammonium', and 'total organics' are retained. However, if we include more than six variables in the model, the coefficient of 'ammonium' decreases in the model; instead, the coefficients of 'nitrate', 'sulfate', and 'chloride' increase.

With a closer look at the seven variables chosen by the Lasso method with "one standard error rule", we found that the top five influential predictors are all atmospheric parameters (Figure 7b), which are expected to be more associated with 'B_s'. Although three climate parameters ('temperature', 'wind direction' and 'wind speed') are selected by the model, their coefficients are close to zero. The left climate variables (relative humidity and pressure) are discarded by the lasso model.

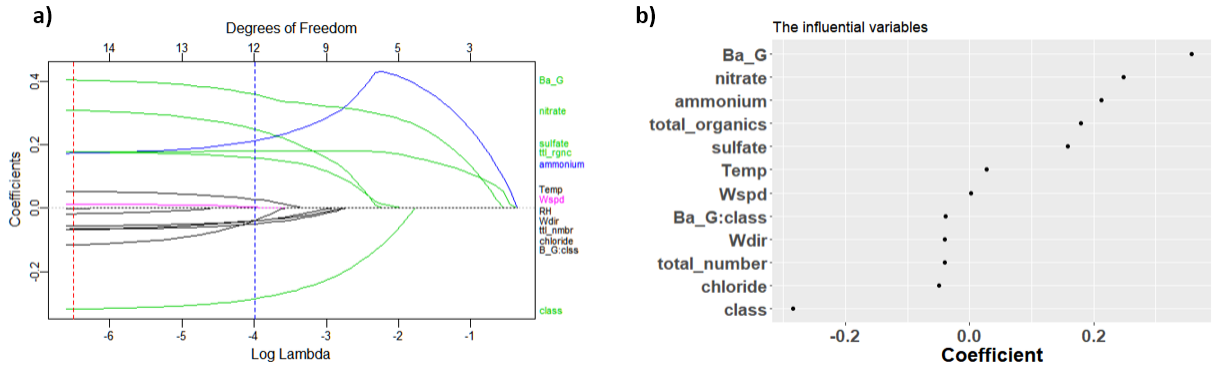

Figure 7. Coefficient paths of regression with lasso penalty

Among the selected variables, 'chloride', 'total number', 'wind direction', 'class' and 'B_a: class' have negative coefficients. Considering the variable of 'wind direction' is a vector in the dataset, we do not attempt to interpret its association with 'B_s'.

Similarly, we visualize the results of ridge model (Figure 8). Unlike the lasso model, the ridge regression does not force any variables to zero. The ridge regression model has pushed the correlated features towards each other (again ammonium, nitrate, sulfate, and chloride). Furthermore, many of the non-important features have been pushed closer to zero (such as 'RH', 'pressure' and 'wind speed').

We would like to point out two features in Figure 8. Firstly, the 'ammonium' does not exhibit increasing trend anymore, confirming that the pattern of 'ammonium' in Figure 7 is due to the feature of lasso

method that seeks for simplicity but sacrifices accuracy (L1 penalty). Secondly, the coefficient of the interaction term ('B_a:class') increases when the log(lambda) increases from -2 to 0.5, and then decrease.

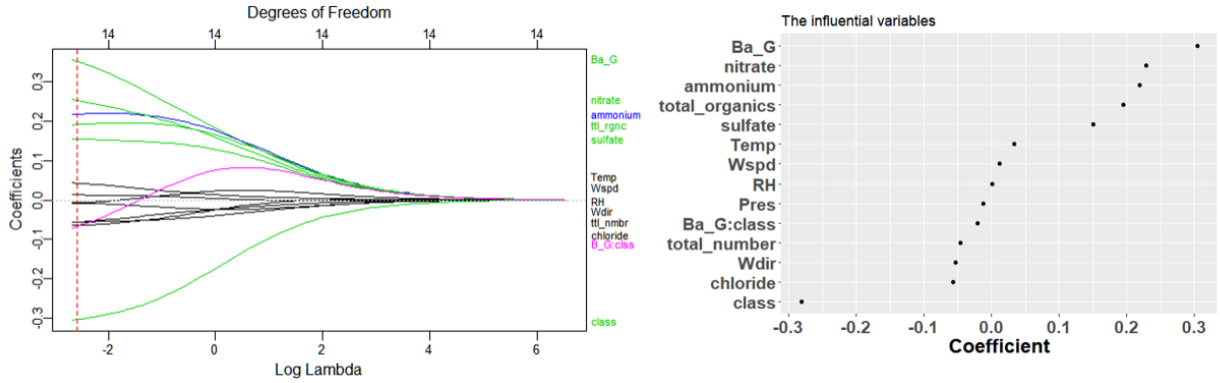

Figure 8. Coefficient paths of regression with a ridge penalty

At this point, among the seven models, 'Best_BIC', forward stepwise', 'backward stepwise' and 'both direction stepwise' yield the same regression model. 'Lasso' and 'ridge' model with the lambda chosen at minimum MSE yield the most complicated model (including all variables). Although five of the models include 12 predictors, the selected predictors are slightly different. The regression results are provided in Table 2.

Table 2. Multiple regression results with after model selection

	Best_Cp	Best_BIC & stepwise	Lasso_w_1se	Ridge
(Intercept)	0.1506 ***	0.1505 ***	0.1374	0.1452
	(0.0083)	(0.0083)		
Ba_G	0.4081 ***	0.4081 ***	0.3579	0.3509
	(0.0094)	(0.0094)		
total_number	-0.0685 ***	-0.0709 ***	-0.0399	-0.0561
	(0.0067)	(0.0066)		
ammonium	0.1657 ***	0.1650 ***	0.2125	0.2172
	(0.0230)	(0.0230)		
chloride	-0.0680 ***	-0.0686 ***	-0.0492	-0.0645
	(0.0061)	(0.0061)		
nitrate	0.3171 ***	0.3180 ***	0.2489	0.2524
	(0.0196)	(0.0196)		
sulfate	0.1806 ***	0.1815 ***	0.1582	0.1548
	(0.0127)	(0.0127)		
total_organics	0.1752 ***	0.1744 ***	0.1791	0.1907
	(0.0094)	(0.0094)		
RH	-0.0204 **	-0.0228 ***		-0.0084
	(0.0067)	(0.0066)		
Pres				-0.0069
Temp	0.0548 ***	0.0576 ***	0.0279	0.0426
	(0.0072)	(0.0071)		
Wdir	-0.0571 ***	-0.0564 ***	-0.0397	-0.0556
	(0.0060)	(0.0060)		
Wspd	0.0132 *		0.0029	0.0128
	(0.0061)			
class	-0.3199 ***	-0.3196 ***	-0.2851	-0.3030
	(0.0118)	(0.0118)		
Ba_G:class	-0.1225 ***	-0.1228 ***	-0.0392	-0.0664
	(0.0119)	(0.0119)		
N	6109	6109	6109	6109
R2	0.7902	0.7900		

4.3.4. Support vector regression

Since support vector regression (SVR) is a non-linear algorithm that project existing features into a high dimensional feature space, there is a lack of statistical explanation of its output. Therefore, in this subsection, we only put MSE on the test set and skip more theoretical analysis.

Table 3. Computed test MSE using support vector regression

Kernel	Polynomial	Radial	Sigmoid
MSE	0.1824	0.1542	2877.966

We accept a 3-degree function as the polynomial kernel, and a hyperbolic function tanh(·) as the sigmoid kernel.

4.4. Validate the models

It should be noted that the model fits in the previous section are calculated using the training data. This means that, the model selection is possibly subject to overfitting and may not perform as well when applied to new data. Therefore, we use the test dataset to calculate prediction error. It turns out that every model has a very similar error anyway (test error rate $\approx$ 0.21). However, test errors of Lasso/Ridge are slightly larger. Table 4 summarizes the detailed test errors.

Table 4. Test MSE computed by each model

Model	**Test MSE**
best_Cp	0.21143
best_BIC	0.21136
Stepwise	0.21136
Lasso_w/ 1*se	0.21975
Ridge	0.21802

Specifically, one may also find that compare with 'Best_BIC' model, 'Best_Cp' model only has an extra variable: 'Wspd'. Using ANOVA test, it turns out the wind speed variable has p-value of 0.03057. If using a rejection level of 0.05, one should consider 'Best_Cp' is better because wind speed is necessary to be included. The models selected by all directions' stepwise methods produced the same results as 'Best_BIC'.

The team also decides to use "one standard error rule" to take a look at each model's cross-validation result.

By observing the left panel in Figure 9, one could see that model 1 (Best_Cp) gives the lowest MSPE. By observing the right panel in Figure 9, within one standard error of model 1, model 2, 3, 4 are all equally simple.

After exploring many model selection criterions, the team finds that none of those criterions can make the decision for the team. So, the team decides to let the science drives the statistics and select the model that most interpretable.

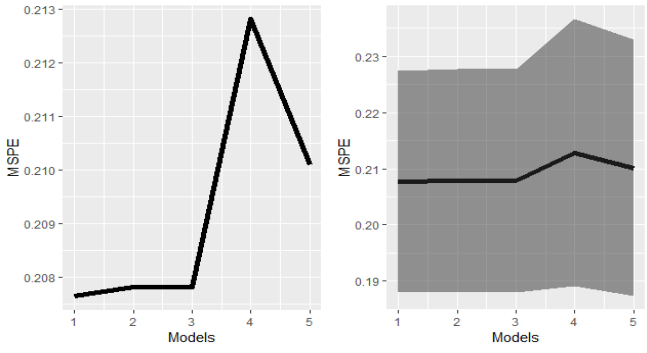

*Figure 9. MSPE of all models. (1: Best_Cp, 2:Best_BIC, 3: forward stepwise, backward stepwise, and both stepwise, 4: Lasso with 1*se , 5: Ridge")*

4.5. Using residual plots to evaluate linear regression models

In the following discussion, we use the model derived by the lasso analysis (the one which is more consistent with common sense) to present our results. The plot of residuals vs. date time order (Figure 10 (a)) shows that residuals are centered around 0, and variance seems to be not constant with time. However, since our data were collected every half an hour, there might be a seasonal component with possible period 48. Figure 10 (b) shows that after transformation over the response variable and scaling over the dataset, residuals seem to have a non-linear trend with fitted values. Also, there are some points with high leverage, noted in red using their ids.

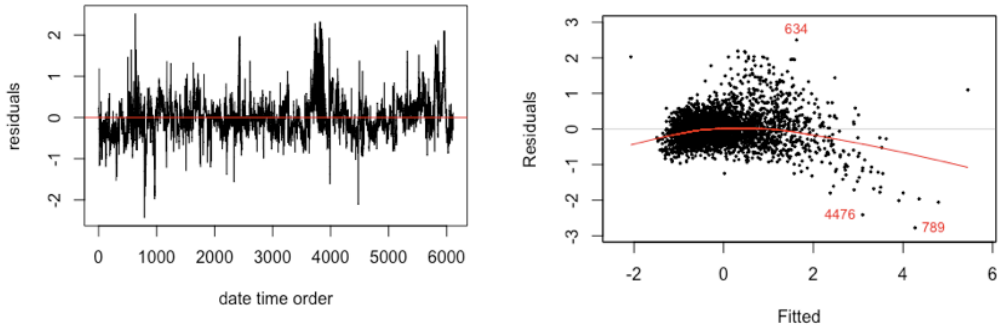

Figure 10. The residual plots of our best model for diagnostics

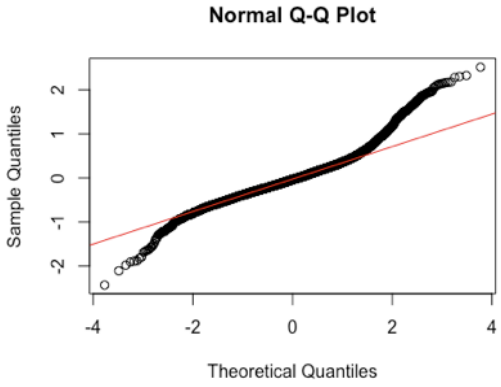

Figure 11. Q-Q plot of the residuals

By checking normality of residuals (Figure 11), we find most points are on the red straight line, however, there are skewness and heavy tails compared to normal distribution. Thus, the normality assumption of linear model might not be satisfied. The reason might be the seasonality of this time series data.

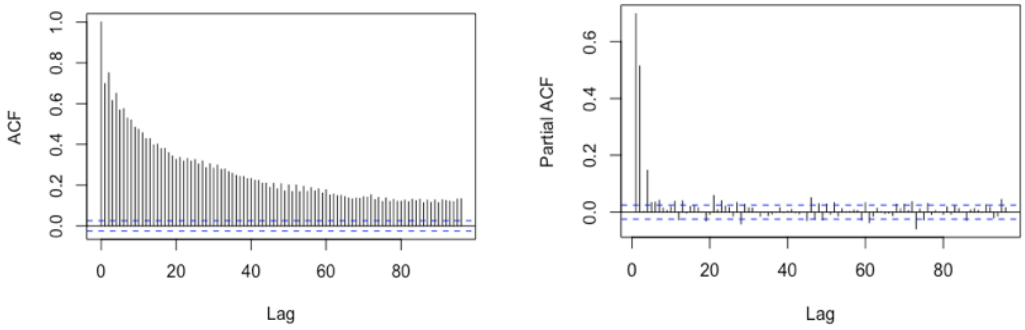

Figure 12. Sample ACF and PACF plots of residuals

To better understand the influence of time, we analyzed sample ACF and PACF plot of residuals (Figure 12). From sample ACF plot, we can clearly see lags decay exponentially, and most of them fall outside 95% confidence bounds, confirming that residuals are time-dependent. Also, in sample PACF plot, the first few lags are out of bounds.

The p-value of Ljung-Box test is extremely small (p=2.2e-16), so we should reject the null hypothesis that residuals are IID noise. Hence, time is an important factor and should be considered in our model.

Through the above plots, we suggested two time series models: ARIMA(4,1,1) and SARIMA $(4,1,1)\times(1,0,1)_{48}$, based on the least AIC/AICC criterion.

After checking the performance of two models' residuals (Figure 13), we find both of them are good fits of our original residuals.

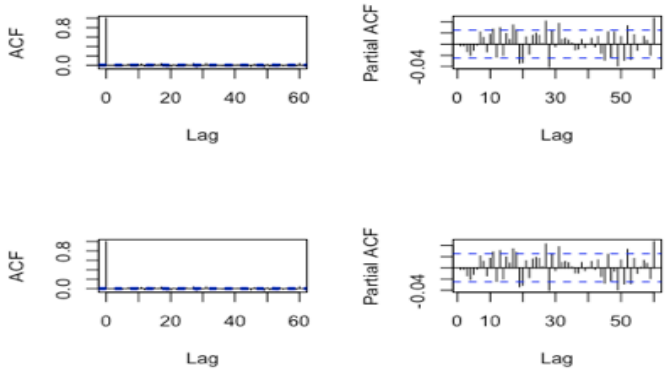

Figure 13. Sample ACF and PACF plots for residuals of two models

Almost all lags are within the confidence bounds in both sample ACF plots, however, there are still a few violations in both sample PACF plots. Results of Ljung-Box test (ARIMA(4,1,1): P=0.8278; SARIMA $(4,1,1)\times(1,0,1)_{48}$: P=0.8209) indicate that we fail to reject the null hypothesis and conclude residuals of two suggested models are IID noise. Also, 95% confidence intervals of all parameters do not contain 0, which means all parameters are significantly different from 0 and models fit good.

Since results are similar, we choose the simple time series model ARIMA(4,1,1) for future analysis, which has the following form:

$$(1-0.32B-0.43B^2+0.06B^3-0.13B^4)(1-B)r_t = z_t - 0.99z_{t-1} \quad \textbf{(2)}$$

where r_t is residuals at time t, B is backshift operator, and z_t~IID(0, 0.08).

5. Conclusion

During this practical case, we firstly illustrate the structures of the data using PCA and then use different regression models learnt in class to predict 'B_s'. Specifically, we used eight model selection techniques to arrive at a reduced model adjudged to be the best. The best lasso model contains 12 explanatory variables for predicting 'B_s' is:
y=0.14+0.36×Ba-0.04×total_number+0.21×ammonium-0.5×chloride+0.25×nitrate+0.16×sulfate+0.18×total_organics+0.03×temp-0.04×wdir+0.003×wspd-0.29×class-0.04×(Ba:class).

We, therefore, advise that the atmospheric research community may adopt this model to predict 'B_s' when the optical measurements of aerosols are unavailable at many of the ground-based networks around the world. The regression model could be beneficial to accurately incorporate regional 'B_s' into a global database, which in turn yields more robust results of climate effects due to scattering aerosols.

6. Individual Contributions

Siyao Cui: Exploring and comparing the distribution of each variable in the dataset for PM1 and PM10 by histograms together with Guanqian. Considering possible transformation methods and influence of outliers. Proposing some supervised learning techniques. Summarizing results of EDA with Qi. Helping to debug code of model selection methods part and focusing on residual diagnostics and time series analysis. Contributing in preparing PowerPoint presentation and report writing.

Kunjie Fan: Explored whether the dependent variable shows significant differences over different months and hours. Performed data transformation analysis for the dependent variable. Performed PCA analysis including PCA scores and PCA loadings analysis. Helped write report and make the presentation.

Guanqian Wang: Explored and compared the distribution of each variable in the dataset for PM1 and PM10 by histograms together with Siyao. Provided general logic procedures and codes/template for model selections.(modified by Hanyang and Siyao) Contributed model evaluations in report writing and PowerPoint presentation.

Qi Zhao: Explored the collinearity and interactions influence in both dataset for PM1 and PM10. Made data preprocessing including deleting missing entries, standardization, splitting dataset for training and testing, merging PM1 and PM10 into one dataset. Made SVR model training and testing.

Hanyang Li: 1. Download the data from the ARM website and preprocess the data (average in 30-min-interval and organize the data for the group); 2. Describe the data and propose the research questions in all submissions; 3. Provide the statistical description of the variables and raise the problem of missing data in the EDA; 4. Output, revise and interpret the statistical results which are computed by Siyao, Guanqian, and Kunjie; 5. Write more than 50% of the submissions and lead the preparation of the slides.

7. References

Boucher, O., 2015. Atmospheric Aerosols. Springer Netherlands, Dordrecht. https://doi.org/10.1007/978-94-017-9649-1

Cappa, C.D., Kotamarthi, R., Sedlacek, A.J., Flynn, C., Lewis, E., McComiskey, A., Riemer, N., 2016. DOE/SC-0185: Absorbing Aerosols Workshop Report.

Jefferson, A., 2011. Aerosol Observing System (AOS) Handbook.

Lelieveld, J., Evans, J.S., Fnais, M., Giannadaki, D., Pozzer, A., 2015. The contribution of outdoor air pollution sources to premature mortality on a global scale. Nature 525, 367–371. https://doi.org/10.1038/nature15371

Malm, W.C., Day, D.E., Kreidenweis, S.M., 2000. Light Scattering Characteristics of Aerosols at Ambient and as a Function of Relative Humidity: Part II—A Comparison of Measured Scattering and Aerosol Concentrations Using Statistical Models. J. Air Waste Manage. Assoc. 50, 701–709. https://doi.org/10.1080/10473289.2000.10464114

Mukai, S., Sano, I., Satoh, M., Holben, B.N., 2006. Aerosol properties and air pollutants over an urban area. Atmos. Res. 82, 643–651. https://doi.org/10.1016/j.atmosres.2006.02.020

White, W.H., Roberts, P.T., 1977. On the nature and origins of visibility-reducing aerosols in the los angeles air basin. Atmos. Environ. 11, 803–812. https://doi.org/10.1016/0004-6981(77)90042-7